GEORGIA INSTITUTE OF TECHNOLOGY — OFFICE OF CONTRACT ADMINISTRATION

PROJECT ADMINISTRATION DATA SHEET

[X] ORIGINAL [ ] REVISION NO. _____

Project No./(Center No.) E-21-611 (R6264-0A0) GTRC/GIT DATE 2 / 9 / 87

Project Director: Dr. C. M. Verber School/Lab Electrical Engineering

Sponsor: UNISYS Corporation

Agreement No.: Research Project Agreement dated 1/22/87

Award Period: From 1/22/87 To 7/22/88 (Performance) 7/22/88 Reports

Sponsor Amount:	New With This Change	Total to Date
Contract Value:	$ 149,992	$ 149,992
Funded:	$ 149,992	$ 149,992

Cost Sharing No./(Center No.) N/A Cost Sharing: $ N/A

Title: Integrated Optical Components for Optical Communications Systems

ADMINISTRATIVE DATA — OCA Contact Brian J. Lindberg X-4820

1) Sponsor Technical Contact:

2) Sponsor Issuing Office:

UNISYS
Defense Products Group
P.O. Box 64525 MS UIL14
St. Paul, Minnesota 55164-0525

Attn: L. A. Prohofsky

Military Security Classification: N/A
(or) Company/Industrial Proprietary: N/A

ONR Resident Rep. is ACO: ____ Yes x No
Defense Priority Rating: N/A

RESTRICTIONS

See Attached N/A Supplemental Information Sheet for Additional Requirements.

Travel: Foreign travel must have prior approval — Contact OCA in each case. Domestic travel requires sponsor approval where total will exceed greater of $500 or 125% of approved proposal budget category.

Equipment: Title vests with none proposed

COMMENTS:

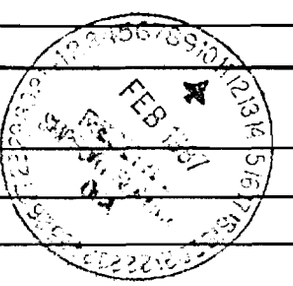

SPONSOR'S I.D. NO. 02.220.000.87N261

COPIES TO:

Project Director
Research Administrative Network
Research Property Management
Procurement/GTRI Supply Services
Research Security Services
Contract Support Div.(OCA)(2)
GTRC
Library
Project File

GEORGIA INSTITUTE OF TECHNOLOGY OFFICE OF CONTRACT ADMINISTRATION

SPONSORED PROJECT TERMINATION/CLOSEOUT SHEET

Date 11/21/88

Project No. E-21-611/R6264-0A0 School/Lab EE
Std. Agreement dtd. 1/22/87
Includes Subproject No.(s) N/A

Project Director(s) C.M. Verber GTRC/GTRI

Sponsor UNISYS/Sperry

Title Integrated Optical Components for Optical Communication Systems

Effective Completion Date: 9/22/88 (Performance) 9/22/88 (Reports)

Grant/Contract Closeout Actions Remaining:

- [ ] None
- [XX] Final Invoice or Copy of Last Invoice Serving as Final
- [ ] Release and Assignment
- [XX] Final Report of Inventions and/or Subcontract:
  Patent and Subcontract Questionnaire sent to Project Director [XX]
- [ ] Govt. Property Inventory & Related Certificate
- [ ] Classified Material Certificate
- [ ] Other

Continues Project No. Continued by Project No.

COPIES TO:

Project Director
Research Administrative Network
Research Property Management
Accounting
Procurement/GTRI Supply Services
Research Security Services
Reports Coordinator (OCA)
Program Administration Division
Contract Support Division (2)
Facilities Management (EHS)
Library
GTRC
Project File
Other

FINAL REPORT

INTEGRATED OPTICAL COMPONENTS FOR OPTICAL COMMUNICATION SYSTEMS

Prepared By:
C. M. Verber
School of Electrical Engineering

Prepared for:
Unisys Corporation

Report Period covered: 1/22/87 - 9/22/88

October 1988

GEORGIA INSTITUTE OF TECHNOLOGY
A UNIT OF THE UNIVERSITY SYSTEM OF GEORGIA
SCHOOL OF ELECTRICAL ENGINEERING
ATLANTA, GEORGIA 30332

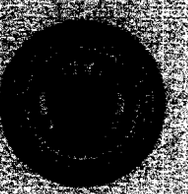

FINAL REPORT

INTEGRATED OPTICAL COMPONENTS FOR OPTICAL COMMUNICATION SYSTEMS

to

UNISYS CORPORATION

from

GEORGIA INSTITUTE OF TECHNOLOGY
School of Electrical Engineering

GEORGIA INSTITUTE OF TECHNOLOGY
SCHOOL OF ELECTRICAL ENGINEERING
ATLANTA, GEORGIA 30332

TELEPHONE: (404) 894-4701

October 24, 1988

Dr. Gerald F. Sauter
Unisys Corp.
P. O. Box 64525, M/S U1L14
St. Paul Minn. 55164-0525

Dear Jerry:

Enclosed are three copies of the final report on our work on the design of an integrated optical switch for multimode communication systems. As you will see, we have finally arrived at a design which we believe will perform the function we were after.

We are still proposing the use of acoustic transducers mounted in pits in the planar waveguide surface, so there will be additional work needed to collect the necessary engineering data on these transducers and on the acoustooptic interaction with multimode guided waves. The required additional steps are outlined in the report.

By an amazing coincidence, one of my students told me that he had been working at Unisys in Huntsville with Michael Beasley (205/837-7610) and that he was convinced that Beasley was looking for a switch for a fiber communication system. If you have no objection, I will call him to see if this is true. If it is, I will ask for your permission to send him a copy of our report.

Bill Hint's student has started to work on collecting the data required to make some initial material selections for a glass substrate for a multimode (or single mode) A-O switch, and our work on the double-diffusion technique for making lenses and other passive components is proceeding well.

We've enjoyed working with you and you colleagues and will keep you posted on our waveguide work.

Sincerely,

Carl M. Verber
Byers Professor

TABLE OF CONTENTS

I. INTRODUCTION 1

II. INTEGRATED OPTICAL DESIGNS FOR NONBLOCKING SWITCHES 2

III. DETAILED DESIGN STUDIES 3

A. General Comments 3

B. Device Design Calculations 7

IV. RECOMMENDATIONS FOR CONTINUED SWITCH DEVELOPMENT 21

A. Achieving a 32 x 32 Switch 21

B. Task Required For Further Switch Development 21

APPENDIX A. A SURVEY OF INTEGRATED OPTICAL SWITCHES A1

APPENDIX B. ACOUSTIC DESIGN STUDIES A2

FINAL REPORT

INTEGRATED OPTICAL COMPONENTS FOR OPTICAL COMMUNICATION SYSTEMS

to

UNISYS CORPORTATION

from

GEORGIA INSTITUTE OF TECHNOLOGY
School of Electrical Engineering

October 8, 1988

I. INTRODUCTION

The program whose results are summarized in this report was initially guided by a Statement of Work which contained the following four tasks:

Task 1. Integrated Optical Designs for Nonblocking Switches

List, discuss and compare the possible integrated optical approaches to the design of a nonblocking switch.

Task 2. Detailed Design Studies

Using the results of Task 1, at least two approaches will be selected for the subject of detailed design studies.

Task 3. Experimental Device Studies

Critical devices and components identified in Task 2 will be fabricated and characterized.

Task 4. Recommendations for Continued Switch Development

This Task will be devoted to planning the next phase of this program. It is assumed that this will deal with the design and fabrication of a 32 x 32 nonblocking switch as well as preliminary work on a WDM system.

As the result of discussions with the Unisys staff early in the program, it was decided that the experimental device studies would be removed from this program and that the constraints of the specific application, that of a switch in an fiber-optic avionics system, should be included at the start. This implies that reliability, maintainability, expandability and low cost are more important than high data-rate capability and leads immediately to the conclusion that multimode systems should be considered in preference to single-mode systems.

II. INTEGRATED OPTICAL DESIGNS FOR NONBLOCKING SWITCHES

A survey of integrated optical switches comprises Appendix A of this report. Switches based on total internal reflection, electrooptic gratings, directional couplers, interferometric principles, magnetic interactions, surface acoustic waves, etc. are described. These are all applicable to single-mode channel or to single-mode planar waveguides. This is due to the fact that the electrooptic and magnetooptic effects which are employed to control the waveguide index, fall off sharply with distance from the surface where the electrodes are located. It was therefore concluded that none of these designs were suitable for the multimode nonblocking switch, since there would be intolerable losses involved in the coupling of multimode fibers into a single-mode integrated optic switch.

It is important to note that if the switch connects single-mode input fibers to multimode output fibers, this conclusion is not valid. In fact, while the connection of an array of single-mode fibers to an IOC is difficult, it can be done with less than

1 dB loss per connection. The connection of multimode fibers to the output of the single-mode IOC is much less difficult and entails negligeable loss. The switch design which we emphasize was conceived for multimode-to-multimode connections. Single-to multimode connection would favor one of the more conventional lithium niobate switches.

In an effort to be fully consistent with the multimode device format suggested by the avionics application, we arrived at an acoustic design which has the advantage of allowing broadcast operation as well as nonblocking switching. This acoustooptic (A-O) switch can also be used as a wavelength-division multiplexing element and it can be adjusted to correct for source wavelength changes which may be due to component replacement or thermal drift.

III. DETAILED DESIGN STUDIES

A. GENERAL COMMENTS

Integrated Optic Multimode Acoustooptic Switch

The integrated optic multimode acoustooptic switch concept is shown schematically in Figure 1. The switch is based upon the principal that a simple lens will cause all rays incident at an angle α to come to a focus at a point on the focal line of the lens which is a distance $f\tan^{-1}\alpha$ from the optic axis. The Figure shows N parallel, equidistant input channels each of which is followed by a beam expander which is required to reduce the diffractive spreading of the beams. Each beam then passes through an acoustic beam which deflects it according to the frequency applied to the acoustic transducer. The acoustic waves are generated by miniature bulk transducers which are mounted in shallow pits which are ion-milled or reactive-ion etched in the waveguide. The transducers are designed to produce an acoustic wave which is not a surface acoustic wave (SAW), but a surface-skimming wave (SSW) whose depth matches that of the multimode optical waves. The pits serve both to position and hold the

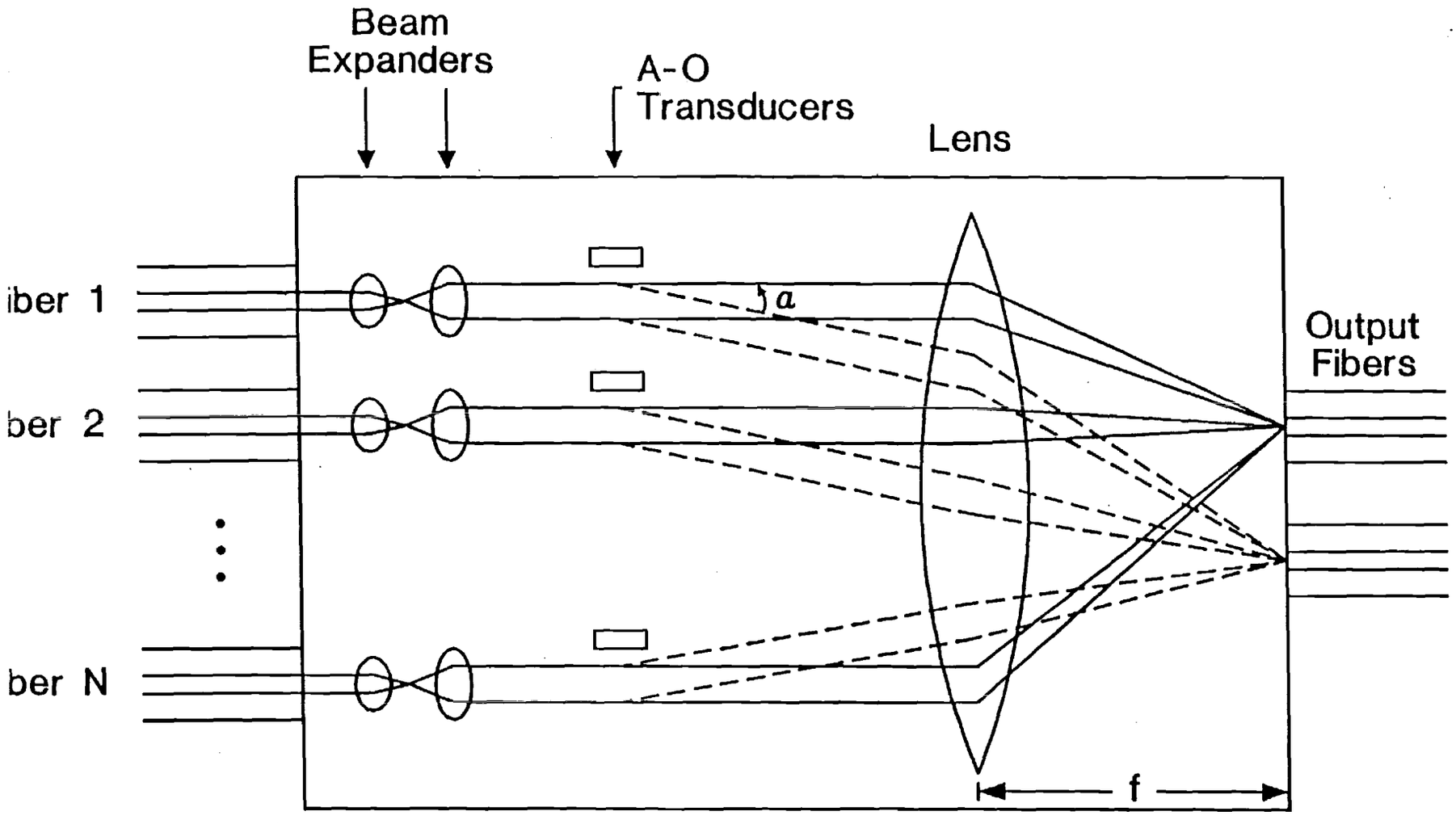

Figure 1. Schematic illustration of the multimode A-O switch concept. N input fibers are butt coupled to the left end of the integrated optical circuit. The beams from the fiber outputs pass through beam-expanding telescopes to reduce diffraction. Each beam then passes through a surface-skimming acoustic wave generated by a set bulk transducers located in pits in the waveguide surface. The Fourier-transform lens then directs each beam to the appropriate output channel. Two sets of output beams separated by the angle α are shown. In normal operation each input beam would be directed toward a unique output channel.

transducers and to block the acoustic wave from adjacent transducers thus preventing crosstalk.

The angle α is determined by the acoustic wavelength Λ and the optical wavelength λ according to the expression

$$\sin \alpha = \lambda/(2\Lambda) \qquad (1)$$

where α is usually written Θ_B, the Bragg angle. The efficiency of the grating is determined by the amplitude of the acoustic wave and can approach 100%. The switching pattern is determined by the frequencies driving each of the transducers.

While operating as a nonblocking N x N switch, each of the A-O transducers would be driven by a single, unique frequency. However, the properties of the acoustooptic (AO) interaction impart a number of interesting and potentially useful properties to the switch. For example:

> If a transducer is driven by N frequencies rather than a single frequency, the optical beam will be split into N beams. In this way a one-to-N or broadcast mode of operation can be achieved. Of course, there is a decrease in the power per output channel.
>
> If there is a drift in laser wavelength due to thermal or aging effects, an appropriate offset can be introduced in the drive frequency so that the deflection angles are preserved.
>
> If lasers of N different wavelengths are used, the switch can be set to deflect all of the inputs into a single output channel. This allows the switch to be used as a multiplexer or demultiplexer in a wavelength-division multiplexing system.

Material Selection

Glass is a natural choice for the waveguide material since it is inexpensive, available in large sizes, can support a variety of passive optical components, can have a fairly high acoustooptic figure of merit and can support multimode waveguides. Not all of the data required to select the optimum glass are available in the literature, so some experimental work may be

required before a selection is made. In the search for the optimum glass the following characteristics must be considered.

+ Optical losses and scattering must be compatible with the application. Losses result from absorption which is a function of glass composition and scattering which is due to a combination of glass composition and the waveguide fabrication technique. Composition effects are usually not a problem in high quality glass. Waveguides are usually made by an ion exchange technique; silver for sodium in sodium-containing glasses is the usual technique. High quality waveguides are obtained by using low-sodium glass since this limits the exchange rate and tends to produce a more uniform silver distribution. Using BK-7 glass, losses of less than 0.1dB/cm have been obtained in our laboratory.

+ The waveguide must be deep enough to match the core diameter of the multimode fiber. This can be done in many glasses by using electric-field assisted ion exchange. This cannot be done in other common substrate materials such as $LiNbO_3$.

+ The index of refraction of the waveguides should be a reasonably good match to the fiber index so low-loss fiber-to-waveguide coupling is possible, and reflections are minimized. This should not be a problem for most glasses.

+ A method must exist for fabrication of the rectangular recesses into which the transducers are inserted. Excellent reactive ion etching results have been demonstrated with some glasses. However, we have been told by the NTT workers who developed the RIE technique that BK-7 does not etch well. Apparently this is related to the low sodium content.

+ The material should have a good acoustooptic figure of merit so that high diffraction efficiency can be obtained with reasonably low acoustic powers.

Two critical points in the selection of a specific glass are A-O figure of merit and the existence of a suitable method for fabricating the recesses required for transducer mounting. In addition, lens formation techniques will have to be evaluated. We have been currently working with a double-exchange procedure in which a planar waveguide is formed by an exchange in a low concentration silver chloride solution and a high-index region is

then formed by exchange through an integral mask in a high concentration solution. This work has thus far been limited to guides which support one or, at most, a few modes. Index ratios exceeding 1.05 have been achieved. Techniques for the fabrication of deep guides, probably using field-assisted exchange will have to be perfected.

B. DEVICE DESIGN CALCULATIONS

The basic switch design problem is to determine the switch geometry and performance in terms of:

N, the number of input and output channels
s, the minimum spacing between input channels
w, the beam diameter in the interaction region
f_o, the center acoustic frequency
Δf, the acoustic bandwidth
F, the lens focal length.

Two approaches to the design are presented. The first is based directly on Figure 1. As will be seen, diffraction problems arise which are overcome by the insertion of an array of beam-expanding telescopes in the input beams. With the beam expansion, the "Focal Plane Design" seems quite feasible. Even so, we have looked at a "Four-F Design" in which the input and output channels are located a distance 2F from the lens. This design produces the desired equality of input and output spot sizes. However, it results in a larger and more complex device, which not only requires two sets of A-O transducers, but which requires an acoustic bandwidth which would be very difficult to attain. Both designs are discussed below.

The Focal Plane Design

Wavelength Choice

In order to carry out the design calculations an operating wavelength must be assumed. Although this system can function

with LED sources, we choose as our starting point the wavelength λ_o = 0.78 μm, which is the nominal output wavelength of the very inexpensive (<$25) diode lasers which are being produced for the compact disk industry.

Acoustooptic Interaction

The switch design is predicated on the assumption that an acoustic wave launched as indicated in Figure 2 will not fan out in depth, and will therefore efficiently overlap the optical beam. The optical waveguide is fabricated by introducing silver ions into the glass thereby increasing its index of refraction. This process also decreases the acoustic velocity and will therefore help to keep the acoustic wave confined to the region of the optical waveguide. The process of exciting surface skimming waves is discussed in some detail in Appendix B.

We must consider both the geometric aspects of the acoustooptic interaction and the power-related aspects. We deal here with the geometric issues; the power-related issues are discussed in Appendix B. The relationship between the Bragg angle Θ_B, the acoustic grating period Λ, and the optical wavelength in the medium λ, was given in Eqn. 1. The geometry is shown in Figure 3. The grating period is related to the acoustic frequency by

$$\Lambda f_a = v_a, \qquad (2)$$

where v_a is the acoustic velocity.

Beam Divergence:

For a focal-plane system, the output spot diameter is equal to F*tan*φ where F is the focal length of the lens and φ is the divergence of the beam on the input side of the lens. Similarly, the maximum linear deflection range in the focal plane is equal to F$\Delta\Theta$ where $\Delta\Theta$ is the angular deflection range of the optical beam due to the A-O interaction. Assuming a diffraction-limited

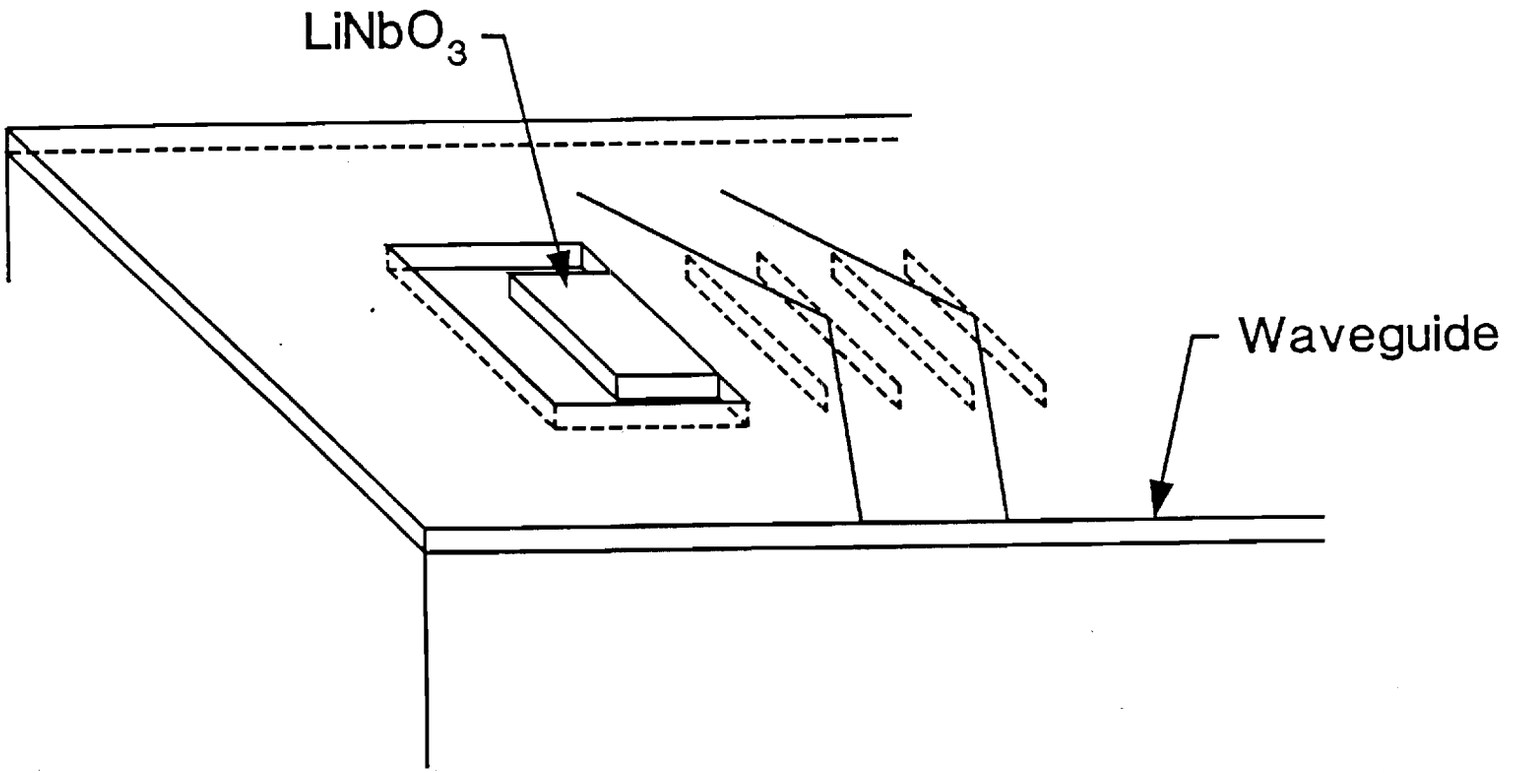

Figure 2. A lithium niobate transducer bonded to the side of a 50 μm deep pit in the waveguide surface. The acoustic wavefronts are indicated by dotted lines and the diffracted optical wave by solid lines. The metalization pattern and leads are not shown.

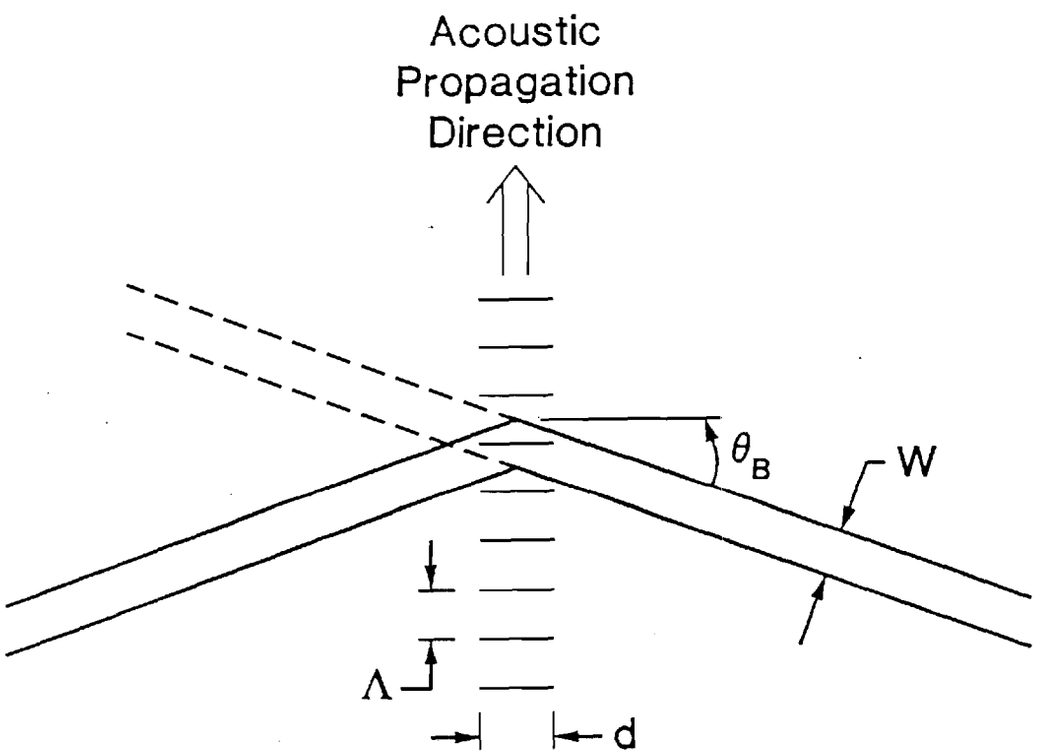

Figure 3. The geometry of the acoustooptic interaction.

input beam, the fundamental limit on the number of Rayleigh-resolved spots into which a given input beam can be directed is

$$N = \Delta\Theta/\varphi_{diff}, \tag{3}$$

the ratio of the angular range of the A-O deflector to the divergence angle of the input beam. We first calculate the angular range of the deflector and then express the minimum acceptable beam divergence in terms of the number of desired output channels.

It is difficult to drive a transducer over a frequency range of more than one octave because of harmonic effects. We assume a one octave range of 200 to 400 MHz and an acoustic velocity of 4×10^5 cm/sec, an average handbook value for several glasses. Table 1 shows the acoustic wavelengths and Bragg angles for a nominal wavelength of 0.78 μm and an index of refraction of 1.5.

TABLE 1. Acoustooptic Parameters

	Λ (μm)	Θ_B (rad)	Θ_B (deg)
f_{min} = 200 MHz	20.0	0.0130	0.745
f_o = 300 MHz	13.3	0.0195	1.117
f_{max} = 400 MHz	10.0	0.0260	1.490

The total angular range available is 0.013 rad.

If we assume that our goal is an 8 x 8 switch, then Eqn. 3 indicates that the beam divergence for Rayleigh-resolved spots is 0.0016 rad. We should do considerably better than this, 0.8 mrad being a suitable goal for φ_{diff} to minimize crosstalk in the output channels.

Beam Width

For a diffraction limited beam the limiting aperture and the diffraction spread are related by

$$\varphi_{diff} = \lambda/W_o = \lambda_o/nW_o, \tag{4}$$

where: λ_o = wavelength in air = 0.78 μm

n = mode index = 1.5

λ = wavelength in the medium = 0.52 μm

w_o = diameter of the limiting aperture.

We have chosen a mode index typical of that which is obtained using glass waveguides. To achieve φ_{diff} = 0.8 mrad implies a beam width of 0.65 mm. This is considerably larger than the 50 μm which is a typical multimode fiber core diameter. However, since φ_{diff} = 10 mrad for a 50 μm spot, we have no choice but to incorporate a beam-expanding telescope for each of the input channels.

Transducer Spacing

For small diffraction angles, the beam width after traversing a path-length p in the planar waveguide is

$$w = w_o + p\,\varphi_{diff}. \qquad (5)$$

If the total path length in the region is 10 mm, the beam will expand to w = 0.6508 mm, so a clear space of 1 mm between transducers will be ample. The transducer should fit in 1 mm-wide slots, so the transducer spacing should be 2 mm.

Acceptance Angle

We examine briefly the variation of diffraction efficiency with departure of the optical beam from Bragg incidence. The diffraction efficiency is a maximum when the optical beam is incident upon the grating at the Bragg angle. The efficiency falls off according to

$$\eta(\delta\Theta) = \eta_{max} sin(\delta\Theta)/\delta\Theta, \qquad (6)$$

where $\delta\Theta$ is the departure of the angle of incidence from the Bragg angle.

The angular separation between the half-power points is approximately Λ/d, where d is the depth of the grating. To maintain less than a 1 dB variation in the diffraction efficiency we will set $\Lambda/2d$ as an acceptable full angular bandwidth. Using the center frequency from Table I, and a 1-mm-wide acoustic beam

(equal to the width of the transducer) we get a 1 dB angle of 0.014 rad. Since this is an order of magnitude larger than the beam divergence calculated above, we can assume uniform diffraction of the beam.

Wavelength Limitations:

The diffraction efficiency also has a wavelength dependence which goes as $[\sin(\delta\lambda)]/\delta\lambda$, where $\delta\lambda$ is the departure from the wavelength which satisfies Eqn. (1) at a particular angle of incidence. It can be shown that the half-power bandwidth is given by

$$\Delta\lambda_{3dB} \approx 2\ \Lambda^2/d, \tag{7}$$

and that the 1 dB wavelength limit is

$$\Delta\lambda \approx \Lambda^2/d. \tag{8}$$

For the same parameters used above, Eqn. 7 yields

$$\Delta\lambda \approx 0.18\ \mu m,$$

which is much larger than the linewidth of any source we might consider using.

Lens Design

The Fourier-transform lens is one of the key components of the switch. We will discuss here the requirements which drive the lens design and the practical limitations on the design.

Lens Diameter: The diameter of the lens is determined primarily by the number of input channels N, and their separation s. Of secondary importance are the beam diameter w, and the width g, of the guard bands which are required to avoid lens edge effects. If we take g = 3 mm and use the previously derived values for the other quantities, we get

$$D = 2g + (N-1)s + w = 20.65\ mm. \tag{9}$$

Focal Length: The collimated beams incident upon the lens can arrive at any of eight angles which are separated by angular intervals $\delta\Theta$. The lens focuses these beams to eight spots in the back focal plane. If the separation between these spots is x,

then the focal length of the lens is

$$F = x/tan(\delta\Theta). \qquad (10)$$

A clear objective is to minimize the focal length of the lens to decrease the overall device size. However, this cannot be done to the extent that it drives the f/no below that which can be reasonably fabricated.

It can be shown that for a given $n = n_1/n_2$, where n_1 is the index of the lens and n_2 is the index of the surrounding medium, that the minimum achievable f/no is given by

$$(f/no)_{min} = 1/2\ ([n + 1]/[n - 1])^{1/2} \qquad (11)$$

We have demonstrated values of n up to 1.05 for single-mode guides which leads to a minimum f/no of f/2.3. We Assume that we can achieve f/2.5 for a lens in a multimode guide. This leads to a focal length of 50 mm and a spot separation x = 93 μm. The distance between the first and the eighth output spot will therefore be 0.651 mm. A set of fanned-out channels to match this array of spots to a set of output fibers can easily be fabricated.

Spot Size: As stated above, the minimum spot size in the focal plane is determined solely by the diffraction spreading of the incident beam. The diameter of the spot is

$$w = F tan\varphi_{diff} \approx F\lambda/w_o. \qquad (12)$$

which in the present case is 40 μm. This is less than the assumed fiber core diameter and should therefore be easily coupled into the fiber.

We have only one other consideration; we must ascertain that the range of angles which must be coupled into the fiber is consistent with the numerical aperture of the fiber. For eight input channels, the inputs are spread over a distance of 7s + 2w. The half-angle describing the range of incident angles at the focal plane is (3.5s + w)/F, or 8.7°. The NA of the fiber is determined by the critical angle which is $\sin^{-1}(n^1/n_2)$ = 81.9° if we assume a fiber with a core index 1% higher than the cladding.

The complement of this angle is 8.1°, just slightly less than the cone which we want it to encompass. These numbers are close enough so that a small change in the index ratio (to 1.0125 rather than 1.0100) or a small reduction of the channel spacing (to 1.8 rather than 2.0 mm) will reverse the situation and allow the entire range of angles to be coupled.

Design Variations

In order to easily investigate the effect of varying the design input parameters, a simple spread sheet was constructed which, more-or-less follows the above design procedure. The spread sheet, which is shown in Figure 4, was constructed using Lotus Symphony but can be reproduced using Lotus 1-2-3. The input parameters and the calculated results are displayed in the Figure. In Step 1, a one-octave rf sweep is assumed and the deflection range is calculated. In Step 3 there is a check to assure that the beam spread is less than three times the grating acceptance angle. This assures approximately uniform diffraction efficiency over the entire beam.

Figure 5 displays the equations used in the calculation both symbolically and in the spread-sheet notation. The latter refer to the rows and columns indicated in Figure 4.

As an example of the utility of the spread sheet we can investigate the diameter and the focal length of the Fourier-transform lens as a function of the number of input and output channels. The results are shown in Table 2. An f/2.5 lens is assumed as this is considered to be feasible using the double-ion-exchange technique.

TABLE 2. Lens Parameters(mm) vs. Switch Capacity

Switch Capacity	Beam Width	Lens Diameter	Focal Length
8 x 8	0.64	20.9	52.3
16 x 16	1.28	47.5	118.7
32 x 32	2.56	131.3	328.3
64 x 64	5.12	421.8	1054.5

A - O SWITCH

1. Calculate the wavelenght in the guide and the total deflection angle on the basis of the source wavelength, mode index, acoustic velocity and drive frequency. Use fu = 2 fl.

INPUT PARAMETERS			CALCULATED RESULTS		
					eqn.
Wavelength-air (um)	lo	0.78	wavelength-wg (um)	l	0.5200 (1)
acustc vel.(cm/sec)	v	4.0E+05			
acustc freq.(MHz)	f		acustc wvlngth(um)	L	
lower	fl	200			20.0000 (2)
center	fo	300			13.3333 (2)
upper	fu	400			10.0000 (2)
mode index	nm	1.50	Bragg angl.(mrad)	thta	
grating depth (mm)	d	1.00	minimum	thmin	13.0003 (3)
			center	tho	19.5012 (3)
			maximum	thmax	26.0029 (3)
			Deflection range	THTA	13.0025 (4)

2. Allowed diffraction spread = (1/2)(range of deflection)/number of channels. Use to calculate minimum beam width.

INPUT PARAMETERS			CALCULATED RESULTS		
number of channels	N	8.00	allowed diff. spread (mrad)	phi	0.8127 (5)
			minimum beam width (mm)	w	0.63987 (6)

3. Check to see if 3*phi < grating acceptance angle.

			acceptance ang.(mr)	dthta	13.3333 (7)
			OK = 1		1
			STOP = 0		------

4. Using accepted value of w determine the transducer spacing asuming 1 mm for transducer pit and 0.4 mm beam clearance.

			beam separation (mm)	s	2.04

5. Calculate the lens diameter using the beam separation and the guard band width g.

lens guard bands(mm)	g	3.00	lens diameter (mm)	D	20.9 (8)

6. Calculate the lens focal lenght assuming f/2.5 lens can be made.

f/no.		2.50	focal length (mm)	f	52.3 (9)

7. Calc. distance between focal spots in focal plane.

			spot spacing (um)	x	97.14 (10)

Figure 4. Symphony spread sheet for the Focal-Plane design.

	SPREAD SHEET FORMULA	EQ. NO.	ALGEBRAIC EQUATION
10	+D10/D16	(1)	l = lo / nm
13	+$D$11/(100*D13)	(2)	L = (10E4 v)/(10E6 f)
14	+$D$11/(100*D14)	(2)	
15	+$D$11/(100*D15)	(2)	
17	@ASIN($J$10/(2*J13))*1000	(3)	thetaBragg = ASIN(l/2L)
18	@ASIN($J$10/(2*J14))*1000	(3)	
19	@ASIN($J$10/(2*J15))*1000	(3)	
20	+J19-J17	(4)	THTA = thmax - thmin
30	(1/2)*J20/D29	(5)	phi = (1/2)THETA/N
32	+J10/(J30)	(6)	w = l / phi
36	+J14/(D17*1000)*1000	(7)	dthta = L /d
44	+J32+1.4		
48	2*D48+(D29-1)*J44+J32	(8)	D = 2g + (N-1)s + w
53	+J48*D53	(9)	f = D * f/no.
57	+J53*J20/(D29-1)	(10)	x = f * THTA / (N-1)

$$\int_0^1$$

Figure 5. The algebraic expressions and the spread-sheet formulas corresponding to Figure 4.

As the number of channels is increased, the lens diameter grows superlinearly since diffraction considerations force an increase in the beam diameters. The lens parameters quickly get out of hand and essentially determine the dimensions of the switch. A 16 x 16 device would seem to be the maximum practical switch. It would have an overall length of about 20 cm and could be expected to have an optical waveguide loss of less than 3 dB.

If we removed the one-octave limitation on the A-O transducers and incorporated transducer arrays so that beam-steering could be accomplished, the pressure on the beam width would be relieved and a 32 x 32 device could be considered.

The effect of the f/no was also investigated for the 8 x 8 switch. The lens diameter remains constant. The effects of increasing the f/no on the focal length and the spot separation are displayed in Table 3.

TABLE 3. Switch Parameters vs. f/no

f/no.	Focal Length (mm)	Spot Separation (μm)
2.5	52.3	97
3.5	73.3	136
5.0	104.6	194
6.0	125.5	233

As can be seen, there is much to be gained in overall device size by using the smallest possible f/no. However even with an f/6 lens the device is not too large and we gain in not having to fabricate a set of channel waveguides to fan out the closely spaced spots to register with the output-fiber array.

The Four-F Design

Another approach to the switch design is based upon the fact that objects a distance 2F from a positive lens are imaged with unit magnification at a distance 2F from the other side of the

lens. The implication is that identical fibers can be used for the input and output arrays without the use of beam-expanding optics on the input end. However, as can be seen in Figure 6, the problem with the 4F design is not the spot size, but the fact that the beams from different input channels hit the 2-F plane at different spots even though their angle of incidence on the lens is the same. They, of course, pass through the same spot on the focal plane so an A-O deflector can be used here to bring the beams (individually) to the same spot on the 2-F plane. The major concerns here are the angular range required of this second deflector set, and the budgeting of space in the focal plane.

Since the unity magnification automatically handles the diffraction problem, the minimum input aperture is determined by the acceptance angle of the acoustic wave. From Eqn. 6 we again get 0.014 rad. The aperture corresponding to a diffraction-limited beam with this divergence is 37 μm, so we are safe with fibers and coupling channels having a 50 μm core diameters. This eliminates the need for the beam expanders required in the focal-plane design.

Focal-Plane Space Budget

Beam Separation. Assuming collimated beams as in Figure 6, it is evident that, if the Θ_1 is the angular separation imparted to two adjacent channels by the A-O deflector, then the resulting two focal spots are separated by a distance

$$y_2 = F \tan \Theta_1, \tag{13}$$

independent of the input beam involved.

Spot Size in the Focal Plane. While we assume that the input beams are diffraction-limited, they are by no means collimated. Assuming 50 μm apertures and a 0.52 μm wavelength, the beam spread due to diffraction is φ = 0.01 rad. The spot size in the focal plane due to this divergence is

$$\delta y_2 = F \tan \varphi = 0.01F. \tag{14}$$

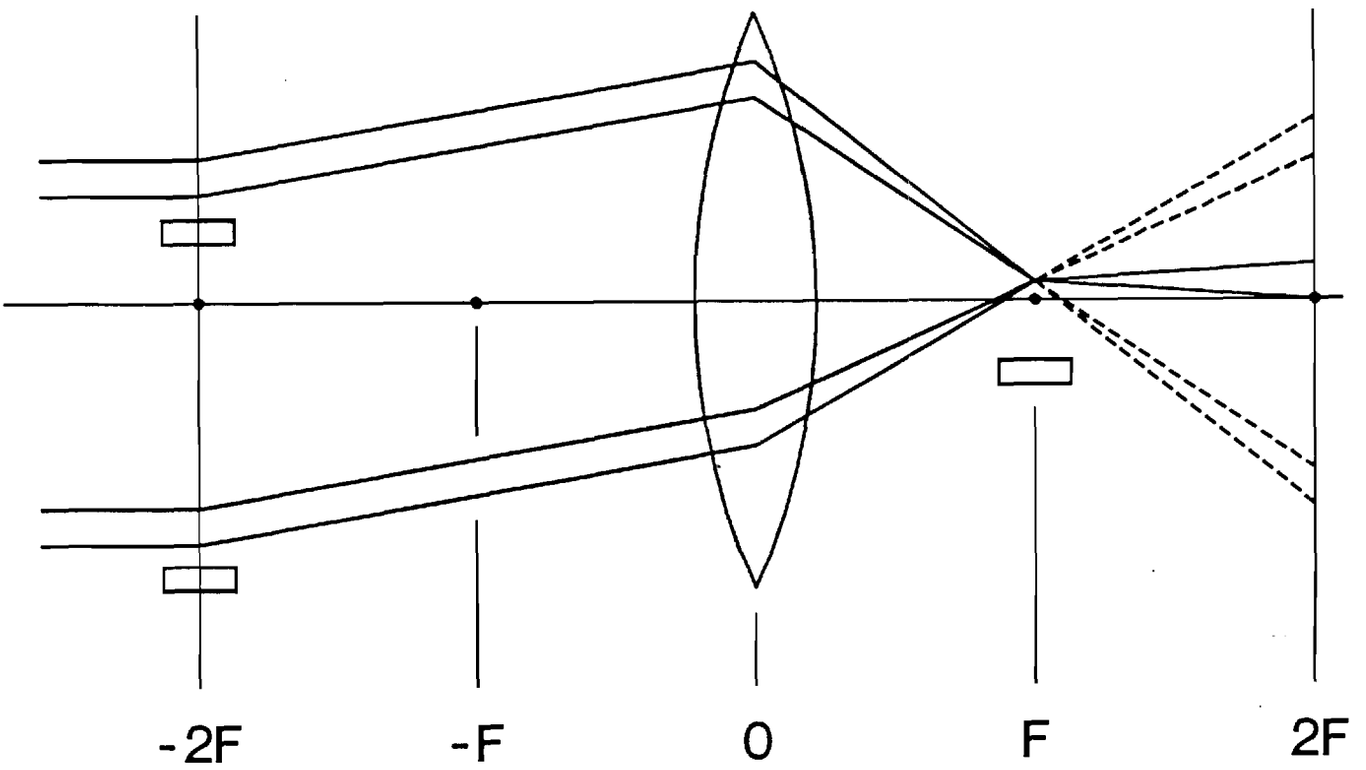

Figure 6. **The four-F design. The first set of A-O deflector are located in the -2F plane. The output channels are in the +2F plane. Two of the N input beams are shown. When deflected at the same angle α in the -2F plane, the beams intersect in the focal plane. A second A-O deflector is then required to bring these beams to a common spot in the output (2-F) plane. There will have to an array of deflectors, one for each output channel. For this drawing, the input beams are assumed to be perfectly collimated.**

Using deflection increments of 0.8 mrad, Eqn. (13) indicates a beam separation of 8 x 10^{-4} F in the focal plane. Clearly we cannot tolerate a beam diameter larger than the beam separation in the focal plane, since we must have room for the second set of A-O transducers between the beams.

A solution to the focal-plane space budget problem might be to increase the deflection angle in the input plane. To get a 2 mm beam separation would require incremental beam deflections of 0.040 rad or a total deflection range of 0.28 rad (16 deg.). We do not believe that this is feasible, and therefore favor the focal-plane design.

IV. RECOMMENDATIONS FOR CONTINUED SWITCH DEVELOPMENT

A. ACHIEVING A 32 x 32 SWITCH

According to the data of Table 2, it is reasonable to think of a monolithic 16 x 16 switch. It should have overall dimensions of about 150 mm x 400 mm (6" x 16") and should therefore be compatible with standard relay-rack packaging. A 32 x 32 switch can be assembled from six 16 x 16 units as shown in Figure 7. However, there are a number of tasks which must be completed successfully before an attempt is made to make even an 8 x 8 or smaller switch.

B. TASKS REQUIRED FOR FURTHER SWITCH DEVELOPMENT

As can be seen with reference to Figure 1, the A-O switch requires beam expanding telescopes, a large Fourier-transform lens, transducers for the production of surface skimming waves which are matched in depth to the multimode optical waveguide, and arrays of butt-coupled multimode fibers. We are currently working, on an internally-funded program, to perfect ion-exchange techniques for lens fabrication in single-mode guides. This work must be extended to multimode guides. We are also planning a

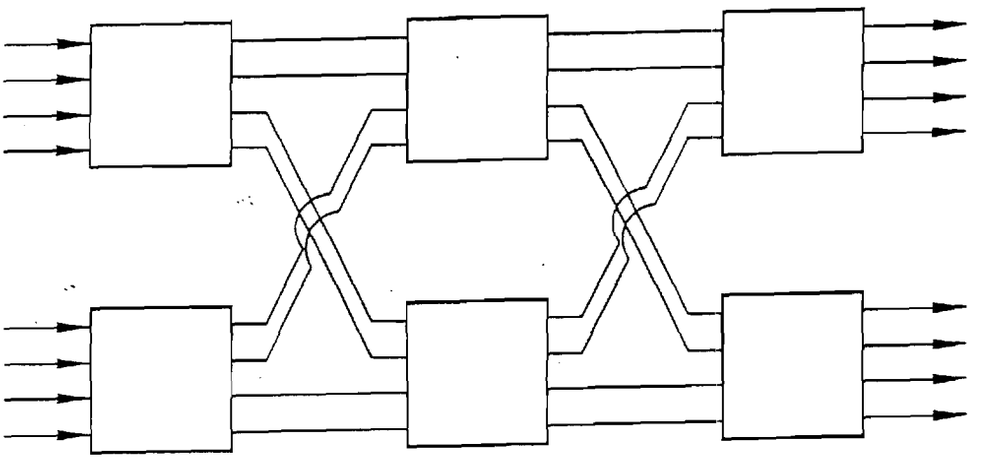

Figure 7. A method for assembling an N x N switching network from six N/2 x N/2 units. The example shows an 8 x 8 nonblocking switch assembled from 6 4 x 4 switch units.

program to investigate the characteristics of the acoustooptic interaction in multimode waveguides.

After preliminary work on the lens and A-O problems it should be possible to select an optimum glass to the A-O switch. It would then be possible to carry out a detailed design study, based upon the glass and waveguide characteristics. This would be followed by a fabrication and testing program.

APPENDIX A

A Survey of Integrated Optical Switches

A. Switches Based on Total Internal Reflection (TIR).

These switches can be made for use in both planar and channel guides. For planar guides, Sheem and Tsai [Pl 1,2] used a guide formed with a "built-in" channel, or strip, of guide with a lower refractive index, as in Fig.1, with electrodes at the edges. An applied field can be used to alter the critical angle, so one can, by adjusting the angle of incidence with zero applied field, switch both into or out of TIR. Response is shown in Fig.2 for the case where the light is initially transmitting and the field switches into TIR. Note that the transmitted light does not reach zero and the reflected light does not appear to reach TIR, probably due to residual tunneling. This kind of switch can not reach zero reflection because of the built-in index difference, but it appears to have only a small residual reflection.

It would appear that there might be real advantage to using the purely electrooptic TIR switches, of the kind discussed below for channel guides.

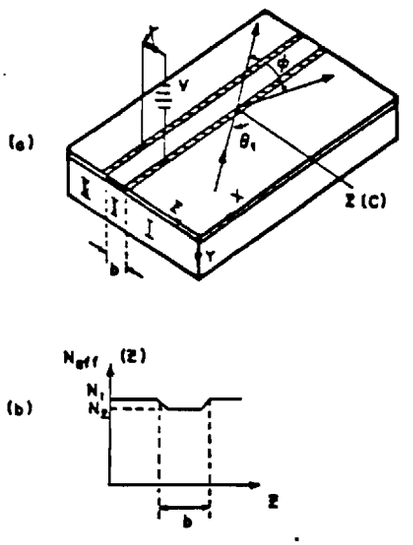

Fig. 1. Guided-light beam switching and modulation using a built-in dielectric channel: (a) device configuration; (b) refractive index profile of the dielectric channel.

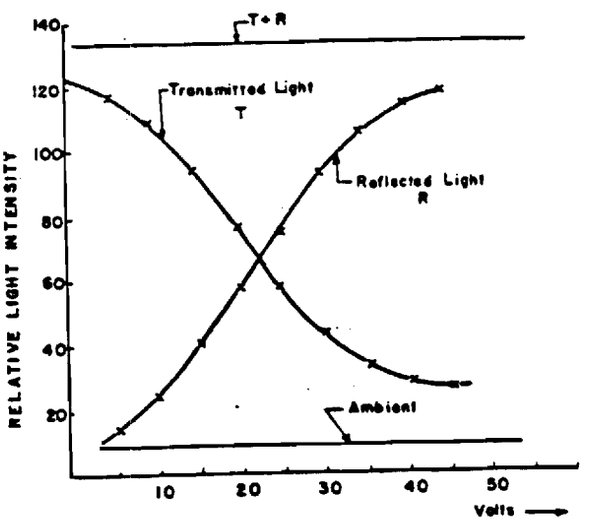

Fig. 2. Transmitted and reflected light intensities vs dc drive voltage.

NOTE: The references have been divided into groups:
"Pl" means the planar guide group, p. 11
"Ch" means the channel guide group, p. 12-13
A third group, "GaAs Technology" is included on p. 14.

For channel guides, both the "built in" [Ch 5,6,10] mirror, altered by an electric field, and the purely electrooptic device are used. Naitoh et al [Ch 5,10] utilize binary branching channels, as in Fig.3, with a mirror along the branch bisector and electrodes to modify the critical angle. Tsai et al [Ch 6] use an intersecting channel (4-port) with electrodes, and sometimes a built-in mirror, placed in the intersection (Fig. 4). The Tsai device operated in the 20-50 Volt region, higher voltages corresponding to lower crosstalk. The Naitoh et al device used much higher voltages in the implemented versions, up to 300 volts; however, it should be noted that their channels separated at five degrees, an extremely large separating angle. It should be possible to reduce the voltages required for both devices, by use of smaller electrode spacings and/or lower separating angles, to quite low values. There are engineering tradeoffs involving drive voltage, speed, crosstalk, and separating angle.

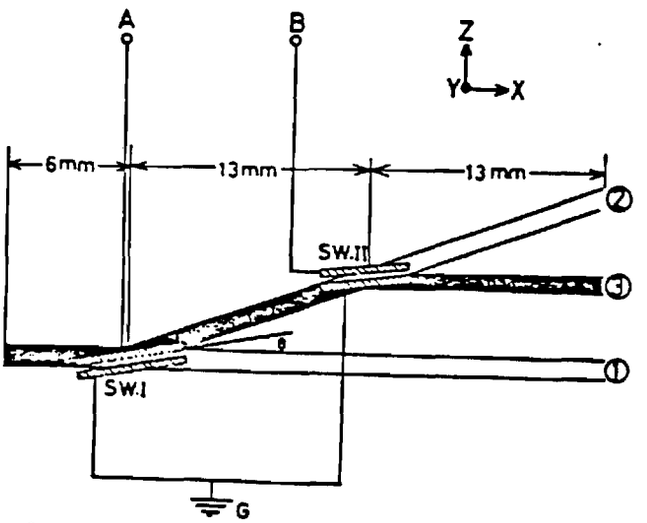

Fig. 3. Basic structure of a mirror type optical switch array. The effective index of the shaded guide is larger than that of the unshaded guide. X, Y, and Z represent the crystal axes of $LiNbO_3$.

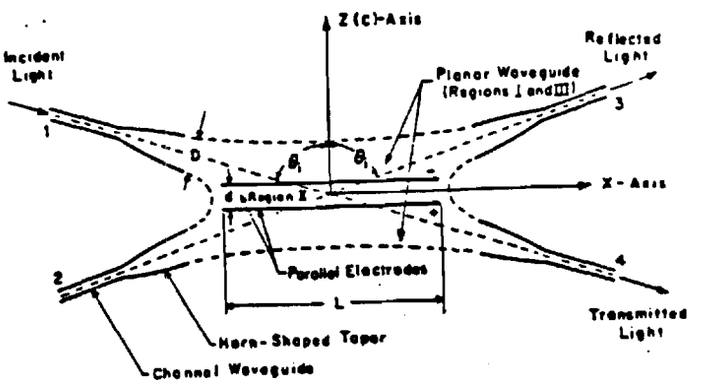

Fig. 4. Configuration of optical channel waveguide double-pole double-throw switch and coupler in Y-cut $LiNbO_3$ substrate.

B. Switches Based on Electrooptic Gratings (EOG).

For planar guides, these switches are very simple to fabricate, consisting only of one or more electrode sets on a planar waveguide. The electrode sets can be interdigital, having a form similar to those used for generation of surface acoustic waves (SAW), Fig.5. With good design, the gratings can be made efficient, upwards of 95%. However, for switching applications, a 5% inefficiency is too large, and steps must be taken to eliminate the undiffracted light from the output channels. This is often done geometrically.Ref.[Pl 3] arranges the elements of a 2x2 switching matrix so that the undiffracted light falls in unused places (Fig.6). It is difficult to see how one can expand this to many channels. Ref.[Pl 9] implements a 1x4 matrix (Fig.7). This might be useful for a TDM demultiplexer.

For channel guides, Chen and Meijer [Ch 4] use a structure similar to that used by Tsai for a TIR switch (Fig.8) to implement a four-port switch. In the implemented device, losses were high, indicating imperfect alignment or mode conversion. Becker and Chang [Ch 2] use a crossing-channel structure (Fig.9) as an element in a (proposed) switch matrix. The single crossing-channel element was implemented and evaluated. Performance was generally good. The switch was compared to the TIR switch of Tsai, discussed above.

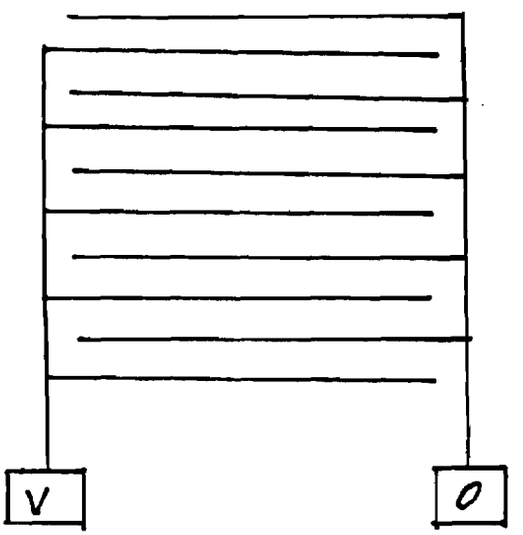

Fig. 5.

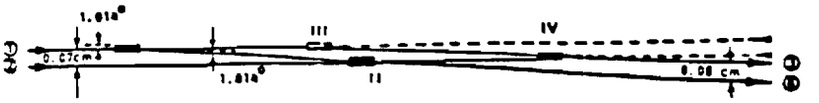

Fig. 6. Beam transformation through the 2 × 2 switching matrix.

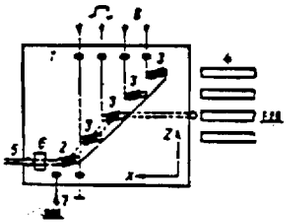

Fig. 7. Schematic diagram of an integrated-optical switching system.

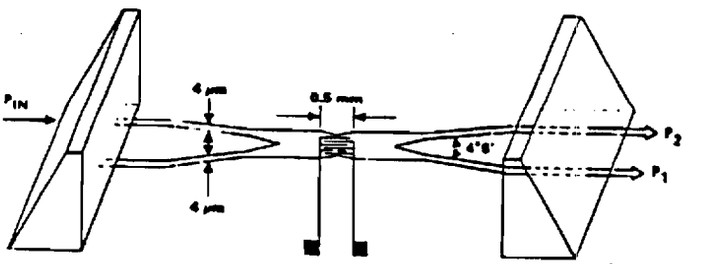

Fig. 8. 4x4 Using EOG

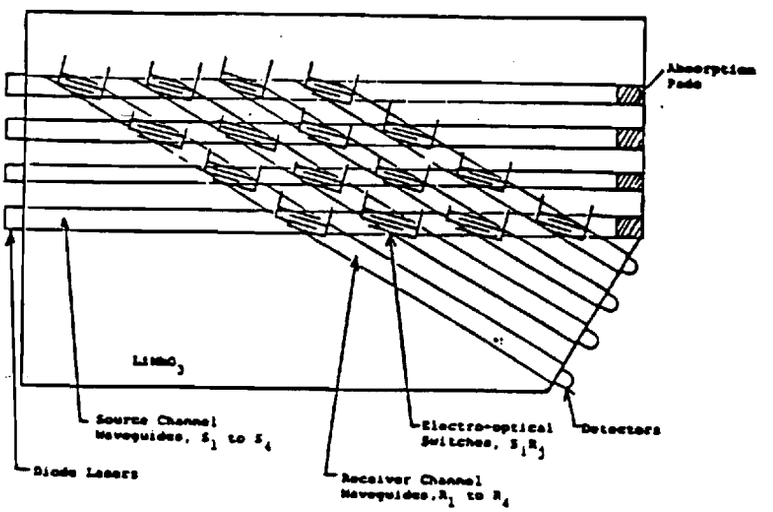

Fig. 9. Illustration of an integrated optical channel waveguide communication bus.

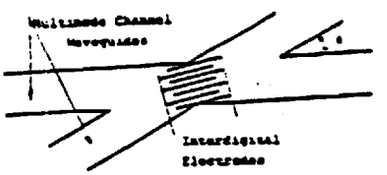

Fig. 9. Crossing channel switch.

C. Switches Based on Directional Couplers (DC).

By far the largest number of switch designs involve the use of directional couplers, with coupling adjusted by use of the electrooptic effect. These are intrinsically channel-guide structures. References [Ch 1,3,7,8,11,and 13-19] in the list for channel guides are concerned with directional couplers.

The most commonly-used coupler switch is the stepped coupler, illustrated in Fig.10. The basic scheme of operation is to alter the synchronism of the coupled guides using the electro-optic effect. It is easy to obtain 100% straight through operation with a single electrode set, but difficult to obtain 100% transfer to the second guide unless the coupling region is exactly the correct length--a serious fabrication problem in integrated optics. By splitting the electrodes, one can accomplish either switch state by using the first set to achieve exactly 50% transfer and then using the second either to complete the transfer or (by reversing the voltages relative to the first set) to reverse it. Very good switching characteristics can be obtained. The drawback to this kind of switch is space--the device length is prohibitively long if several of them are to be combined into a matrix.

Ogiwara and Yamamoto [Ch 1] use a three-channel coupler (Fig.11) to achieve a 3x3 switch. The use of a 3x3 as a switching-matrix element is motivated because the number of switch stages required to exchange a given number of channels is reduced when larger switches are used. An example: 7 stages of 3x3 can exchange 81 channels while 12 stages of a 2x2 are needed to exchange 64 channels (example from ref. Ch 1). The authors propose the switch and present numerical calculations; no known experimental data are available. Ogiwara [Ch 8] has given a separate theoretical discussion of control problems in this switch. Mitsunaga et al [Ch 14] propose a 3-branched waveguide (Fig.12) as a component in the fabrication of a 4-port switch. Some experimental work is also presented. Their guides were not monomoded, so the extinction was not as good as desired, but the data are impressive.

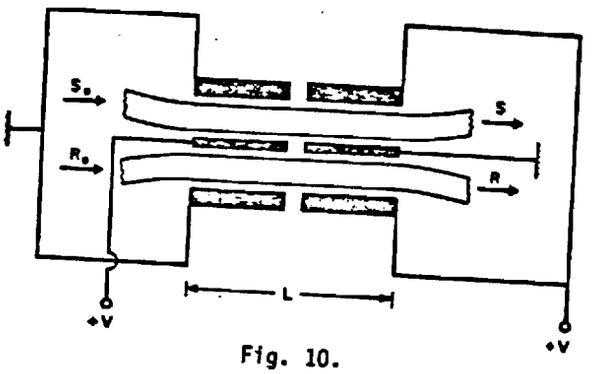

Fig. 10.

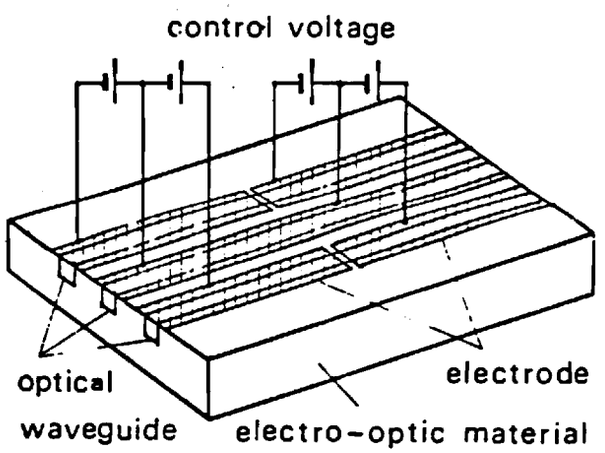

Fig. 11. 3 × 3-switch element plan.

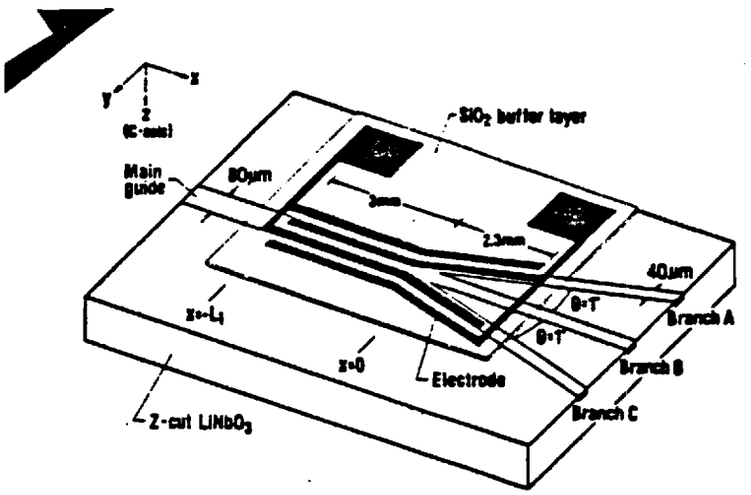

Fig. 12. Schematic diagram of an optical multimode 3-branched waveguide fabricated in Ti-diffused Z-cut $LiNbO_3$, where the main guide and each branch are 80 and 40 μm wide, respectively, with the branching angle of $\theta = 1°$.

Campbell and Li [Ch 7] have designed a multimode switch that they call a MONGOOSE. Devices have been fabricated and evaluated, with good results. The switch uses waveguide imaging. In addition to these switch types, there are several reports of directional-coupler switches fabricated in GaAs. This technology, which may someday allow monolithic integration of integrated optical circuits complete with sources and detectors, is not now in a state where many practical applications are at hand, but developments are taking place. The bibliography includes several papers on this material.

D. Switches Based on Interferometric Principles (IP).

An interferometric switch operates in the general manner outlined by Zernike [Ch 9] and illustrated in Fig.13. The basic idea is applicable to both planar and channel guides. Input light is split into two equal parts; one part is phase shifted; then the two parts pass on to a second mixing stage (coupler or beam combiner). If the phase shift is zero, the light is recombined into one output direction. If it is, then the light all passes into the second output direction.

Implementation of an interferometric switch in a planar guide could be accomplished using surface gratings or electrooptic gratings for beam splitters and combiners and a set of electrodes located in one path to produce the phase shift. Better control over diffraction can be achieved by using channel guides. In either case, the switch is basically a Mach-Zehnder interferometer. While interferometers have been used for other purposes, little has been reported about their use as switches.

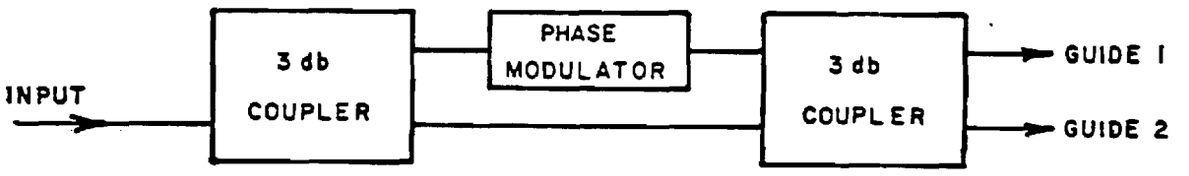

Fig. 13.

E. Switches Based on Crossing Channels and Electrooptic Effect (CC).

A number of workers have investigated the question of how to utilize channel waveguides that simply cross one another. The difficulty in channels that cross at small angles is that the input guides will couple to one another as they approach the intersection, leading to strong crosstalk (equal power division). For large crossing angles, the light "sees" an effectively infinite width guide at the intersection; so losses are very high. One solution to this is to make the intersection region have a higher index, so that, at least at large intersecting angles, the light is confined to the intersection. For small angles, this leads to possible TIR at the intersection edge, and the problem is aggravated. The TIR switches for channel guides that were discussed earlier can be adapted for use in crossing channels (without enhancement of the intersection index), as can the electrooptic gratings. Indeed, as discussed earlier, the paper by Becker and Chang [Ch 4] investigated both of these devices.

F. Switches Based on Magnetic Interactions (MI).

Magnetic interactions with waveguided light are relatively little investigated because of the limited materials for the waveguides. Tienetal [Pl 8] have investigated magnetooptic interactions using single-crystalline ferrimagnetic films of $Y_3Ga_{0.75}Sc0.5Fe_{3.75}O12$ (Yttrium-Gadolinium-Scandium ferrite) as waveguide. A switch that utilizes the mode conversion from TE to TM light due to the Faraday effect in an applied field. The field is applied using the serpentine electrodes shown in Fig. 14 from that paper.

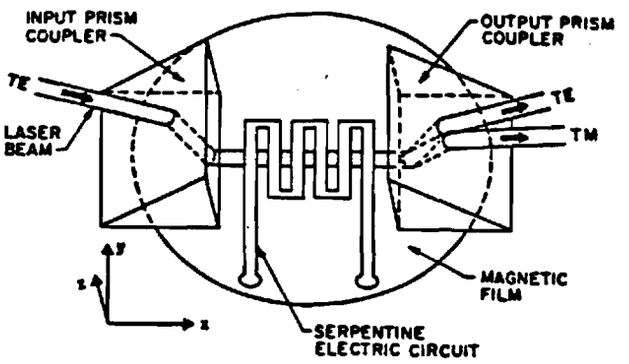

Fig. 14. Schematic drawing of the film-waveguide magneto-optical switch in operation. As the current in the serpentine circuit is on and off, the light beam emerging from the output prism coupler switches between two different directions.

TE and TM light have different propagation constants, and so emerge from the prism coupler in different directions, and are detected separately. The input light is all TE, so the modulation from the mode conversion can be used for a switch. The switch can operate to GHz frequencies. The questions of configurations to make purely thin-film versions and how to array the switches were not addressed in the early paper. Interest in magnetooptic interactions for switching appears to have disappeared as attention of workers was concentrated on electrooptic materials.

G. Switches Based on Other Principles (OP).

Here, we discuss a few miscellaneous switch types that are not easily classified. Favre and Rivoallan [Pl 4] describe an electrooptic modulator/switch formed in z-cut Ti:LiNbO3. The device is shown in Fig.15. The applied field, through the large electrooptic coefficient, r33, causes a region of increased refractive index under one elctrode and a region of decreased inedx under the other. The region of increased index forms a "guide", i.e., a region where the guided wave tends to move. Depending on the sign of the applied potential, the light is moved under one or the other of the electrodes. At the end of the electrode, the light encounters one or the other of the waveguides delimited by the triangular metallic overlays, and is guided in different directions.

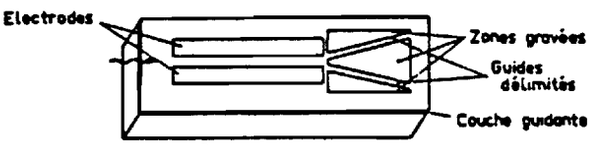

Fig. 15. Schéma du commutateur.

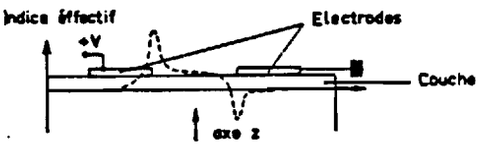

Fig. 15. En pointillé, variation d'indice obtenue dans la couche lorsqu'on applique une tension sur les électrodes.

A paper by Voitenko and Red'ko [Pl 7] discusses an unusual switch design [Fig. 16]. It is a 1x3 switch utilizing a planar Ti:LiNbO3 waveguide. The central portion of the output of the planar guide--the section that would receive the unperturbed input light--becomes a channel guide over some region, and the channel is interrupted over an 0.8 mm length section. The shape of the mask that prevents Ti deposition over the nonguiding region creates a 50 um-to-5 um horn, so that the channel can be easily excited. The input light can be deflected upwards or downwards 2.2 degrees by TIR electrodes. When switched to these output directions, the leakage light (undeflected light) is dumped into the substrate by the interruption in the channel guide. When the undeflected light direction is desired, electrodes acound the interruption restore the guiding and light is correctly output to this channel. Since the light that is "dumped into the substrate" is, in fact, converted into radiation modes, there is still some output in the central channel when the other channels are activated. This amounted to -16 dB. This device does not appear to be easily arrayed, but, for small switching matrixes, it may be useful. The ingenious way of eliminating unwanted light in the central channel is itself of note. Terui, Kobayashi and Noda [Pl 6] discuss a 2x2 switch of almost bizarre design in that it used a movable dielectric chip.

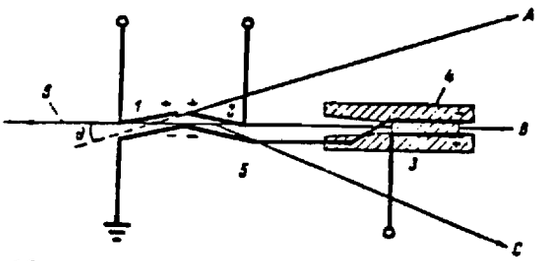

Fig. 16. Diagram of the three-channel electrooptic waveguide commutator switch: 1, 2, 3) electrooptic cells; 4) nonwaveguide region; 5) planar optical waveguide; 6) light beam.

The design is illustrated in Fig. 17. An optical waveguide has a region of lowered index. In this case, the guide was Ta_2O5 sputtered onto SiO_2. The region of lowered index was created by CO_2-laser irradiation, and had a Gaussian index profile. A chip of dielectric material was placed a small distance above the guide/lowered-index stripe/guide composite. Since it had a higher index than the guide, the effective index of the guided mode is a sensitive function of the chip-guide gap width, and the effect on the lowered-index region was stronger than its effect on the guiding region. Light entering at a small angle into the lower-index region would be turned back by the index variation, provided the chip-guide gap was sufficiently large. However, if the chip was brought close enough, this TIR is spoiled and the light tunnels through. Extensive experimental data are presented, including data on the assembly of four of the elements into a 2x2. Insertion losses in the four switching paths range from 2.9 to 6 dB, and crosstalk from 12.5 to 28.1 dB.

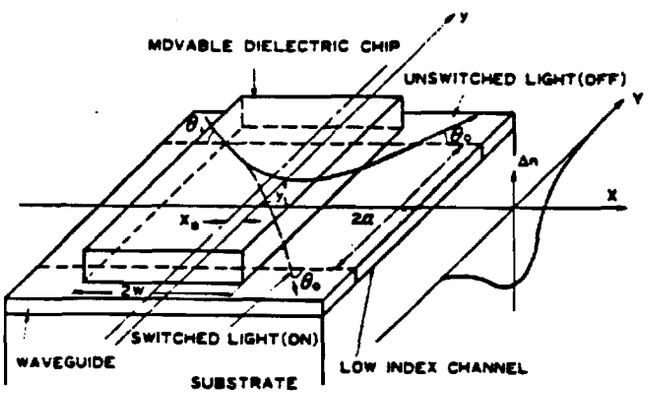

Fig. 17. Structure of the TIR waveguide switch. The $2W$ width movable dielectric chip is set at $(x_0, 0)$ on the built-in low-index channel with a Gaussian index profile. Input light with angle θ_i is totally reflected with the turning point $(0, y_t)$ at the OFF state.

SWITCHES IN PLANAR WAVEGUIDES

1. Sang K. Sheem, "Total Internal Reflection Integrated-Optics Switch: A Theoretical Evaluation", Appl. Opt. 17, 3679-3687 (1978).

2. S.K. Sheem and C.S. Tsai, "Light Beam Switching and Modulation Using a Built-in Dielectric Channel in LiNbO3 Planar Waveguide", Appl.Opt. 17, 892-894 (1978).

3. Elisabeth M.Philipp-Rutz, Robert Linares, and Mike Fakuda, "Electrooptic Bragg Diffraction Switches in Low Cross-Talk Integrated-Optics Switching Matrix", Appl.Opt. 21, 2189-2194 (1982).

4. F.Favre and L.Rivoallan, "Modulateur et Commutateur Electrooptiques", Opt.Comm. 24, 139-142 (1978).

5. Kazuhiko Yamanouchi, Masaski Yasumoto and Kimio Shibayama, "Optical Switching Device Using Leaky Surface Wave", IEEE J.Quantum Electron. QE-14, 863-865 (1978).

6. Hiroshi Terui, Morio Kobayashi and Junichi Noda, "Optical Waveguide 2x2 Matrix Switch Using Dielectric Chip Motion", Appl.Opt. 21, 1979-1984 (1982).

7. I.G. Voitenko and V.P. Red'ko, "Three-Channel Electrooptic Waveguide Commutator Switch", Sov.Tech.Phys.Lett. 7, 178-179 (1981).

8. P.K.Tien, D.P.Schinke and S.L.Blank, "Magneto-Optics and Motion of the Magnetization in a Film-Waveguide Optical Switch", J.Appl.Opt. 45, 3059-3068 (1974).

9. A.M. Belin, BV.N. Ryabokon' and K.K. Svidzinskii, "Integrated-Optical Switching System", Sov.J.Quantum Electron. 10, 249-250 (1980).

SWITCHES IN CHANNEL WAVEGUIDES

1. H. Ogiwara and H. Yamamoto, "Optical Waveguide Switch (3x3) for an Optical Switching System", Appl.Opt. 17, 1182-1186 (1978).

2. R.A. Becker and W.S.C. Chang, "Electrooptical Switching in Thin Film Waveguides for a Computer Communication Bus", Appl. Opt. 18, 3296-3300 (1979).

3. R.C. Schmidt and L.L. Buhl, "Experimental 4x4 Optical Switching Network", Electron.Lett. 12, 575-577 (1976).

4. B. Chen and C.M. Meijer, "Bragg Switch for Optical Channel Waveguides", Appl.Phys.Lett. 33, 33-35 (1978).

5. H. Naitoh, S.Noda, K.Muto and T.Nakayama, "Mirror-Type Optical Switch Array", Appl.Opt. 17, 3975-3978 (1978).

6. Chen S. Tsai, Bumman Kim and Fathi R. El-Akkari, "Optical Channel Waveguide Switch and Coupler Using Total Internal Reflection", IEEE J.Quantum Electron. QE-14, 513-517 (1978). TIR

7. J.C. Campbell and Tingye Li, "Electro-Optic Multimode Waveguide Switch", Appl.Phys.Lett. 33, 710-712 (1978). DC, Multimode

8. H. Ogiwara, "Optical Waveguide 3x3 Switch: Theory of Tuning and Control", Appl.Opt. 18, 510-515 (1979).

9. JF. Zernike, "Integrated Optics Switch", Topical Meeting on IO, Paper WA-5 (19??).

10. H. Naitoh, K. Muto, and T.Nakayama, "Mirror-Type Optical Branch and Switch", Appl.Opt. 17, 101-104 (1978)

11. S.I. Bozhevol'ni, K.S.Buritskii, E.M. Zolotov, A.M.Prokhorov and V.A.Chernykh, "Investigation of an Electrooptic Modulator Formed from Coupled Channel Diffused Waveguides in LiNbO3", Sov. J. Quantum Electron. 12, 1165-1168 (1982).

12. Richard A. Soref and Arthur R. Nelson, "Compound Optical Crosspoint With Low Crosstalk", Appl.Opt. 16, 3223-3227 (1977).

13. K. Mitsunaga, K.Murakami, M.Masuda and J.Koyama, "Optical LiNbO3 3-Branched Waveguide and its Application to a 4-Port Optical Switch", Appl.Opt. 19, 3837-3842 (1980).

14. H. Kogelnik and R.V. Schmidt, "Switched Directional Coupler with Alternating (delta-beta)", IEEE J.Quantum Electron. QE-12, 396-401 (1976).

15. Pascal Thiolouse, Alain Carenco and Robert Guglielmi, "High-Speed Modulation of an Electrooptic Directional Coupler", IEEE J.Quantum Electron. QE-17, 535-541 (1981).

16. R.C. Alferness, N.P. Economou and L.L. Buhl, Fast Compact Optical Waveguide Switch Modulator", Appl.Phys.Lett. 15, 214-217 (1981).

17. L.J. Du and Chin-Lin Chen, "Stepped Switched Optical Directional Couplers with Unequal Section Lengths", SPIE Conference Proceedings 176, 36-40 (1979).

18. Osami Mikami and Sakae Xembutsu, "Coupling-Length Adjustment for an Optical Directional Coupler as a 2x2 Switch", Appl.Phys. Lett. 35, 38-40 (1979).

19. A. Neyer, "Electro-optic X-Switch Using Single-Mode Ti:LiNbO3 Channel Waveguides", Electron.Lett. 19, 553-554 (1983).

GaAs TECHNOLOGY

1. J.C. Campbell, F.A. Blum, D.W.Shaw and K.L.Lawley, GaAs Electro-Optic Directional Coupler Switch", Appl.Phys.Lett. 27, 202-205 (1975)

2. F.J. Leonberger, J.P.donnelly and C.O.Bozler, GaAs p+n-n+ Directional-Coupler Switch", Appl.Phys.Lett. 29, 652-654 (1976).

3. F.J. Leonberger and C.O.Bozier, "GaAs Directional-Coupler Switch with Stepped --- (delta-beta) Reversal", Appl.Phys.Lett. 31, 223-226 (1977).

4. J.C. Shelton, F.R.Teinhart and R.A.Logan, "Single-Mode GaAs-AlxGa1-xAs Rib Waveguide Switches", Appl.Opt. 17, 890-891 (1978).

5. A. Carenco, L.Menigaux and Ph.Delpech, "Multiwavelength GaAs Rib Waveguide Directional-Coupler Switch with `Stepped (delta beta)' Schottky Electrodes", J.Appl.Phys. 50, 5139-5141 (1979).

6. J.C. Shelton, F.K.Reinhart and R.A.Logan, "Rib Waveguide Switches with MOD Electrooptic control for Monolithic Integrated Optics in AsAs-AlxGa1-xAs", Appl.Opt. 17, 2548-2555 (1978). DC

7. A.R. Reisinger, D.W. Bellavance and K.L. Lawley, "GaAlAs Schottky Directional Coupler-Switch", Appl.Phys.Lett. 31, 836-838 (1977).

ANCILLIARY PAPERS

1. H. Yamamoto, M.Yokoyama, H.Ogiwara and M.Yoshida, "Large-Scale and Low-Loss Optical Switch Matrix for Optical Switching Systems", J.Opt.Commun. 1, 74-79 (1980).

2. R.C. Alferness, N.P. Economou and L.L Buhl, "Picosecond Optical Sampling Technique for Measuring the Speed of Fast Electro-Optic Switch/Modulators", Appl.Phys.Lett. 37, 597-599 (1980).

3. Junichi Noda, Masaharu Fukuma and Osamu Mikami, "Design Calculations for Directional Couplers Fabricated by Ti-Diffused LiNbO3 Waveguides", Appl.Opt. 20, 2284-2290 (1981).

4. R.A. Steinberg and T.G. Giallorenzi, "Performance Limitations Imposed on Optical Waveguide Switches and Modulators by Polarization", Appl.Opt. 15, 2440-2453 (1976).

5. R.A. Steinberg, T.G. Giallorenzi and R.G. Priest, "Polarization-Insensitive Integrated-Optical Switches: A New Electrode Design", Appl.Opt. 16, 2166-2170 (1977).

6. R.A. Soref and L.R. Schissler, "Crosstalk Reduction in Optical Switching", Appl.Opt. 14, 2559-2560 (1975).

7. C.S. Tsai and P. Saunier, "New Guided-Wave Acousto-Optic and Electro-Optic Devices Using LiNbO3", Ferroelectrics 10, 257-261 (1976).

APPENDIX B

Acoustic Design Studies

Two designs were considered in this feasibility study. One was an IDT surface transverse wave (STW) technique [1]-[4] and the other was a modified edge-bonded transducer technique [5]-[7]. In both of these approaches the acoustic wave is a horizontally polarized shear which is bound to the surface albeit not as tightly as for conventional surface acoustic waves (SAW). For standard integrated optics acoustooptic modulators, the optical signal must interact with the SAW within an acoustic wavelength of the surface. If one desires for the acoustooptic interaction to take place over considerable depth, as is the case herein where we are dealing with a multimode waveguide, one has to use a low frequency SAW and hence limit the achievable bandwidth of the device. The alternative selected here is to impose acoustooptic interaction between the optical signal and an acoustic wave which extends further into the surface than does the SAW. The particle displacement profile for such an acoustic wave is shown in Figure 1 where it is seen that the wave decays much more slowly into the substrate than for a SAW.

Over the past ten years there has been slowly growing interest in STW devices as an alternative to SAW devices in some applications. For these STW devices, an IDT is used to generate the a surface skimming bulk wave (SSBW) and a groove or metallic grating is used to trap the wave and convert it to an STW. By proper design of the grating the penetration depth of the STW can be controlled. One of the advantages of the STW devices is that the wave velocity is higher thereby making them easier to

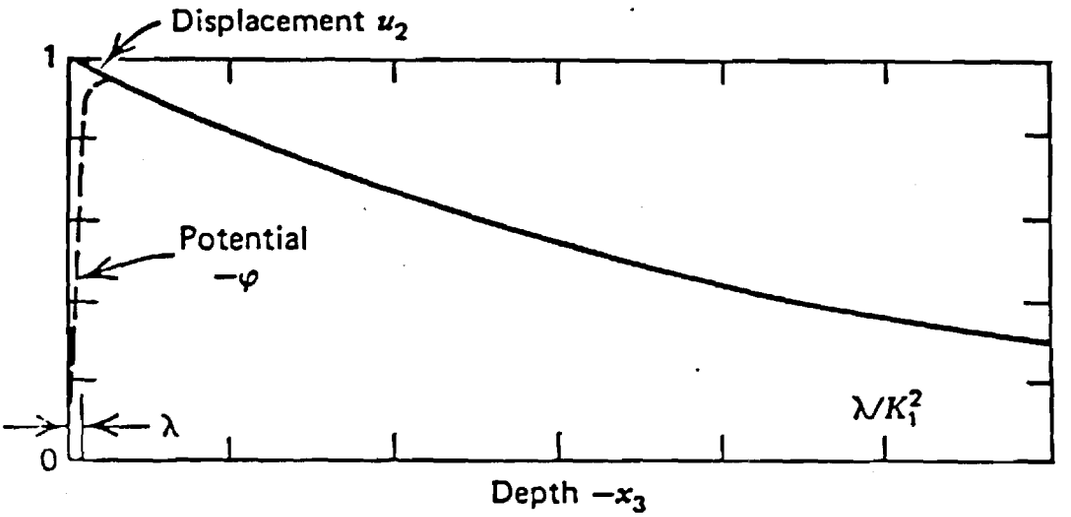

Figure 1: Particle displacement profile for an STW or Bleustein-Gulyaev wave

fabricate with photolithography techniques. In addition, the STW devices have superior temperature stability and are hence very useful for resonator applications [3]. The principal shortcoming of these devices for the integrated optics application proposed herein is the low fractional bandwidth and relatively high insertion loss. A delay line was reported on ST-Quartz which had an insertion loss of 23dB and a fractional bandwidth of 0.9% [8]. A SAW device on ST-Quartz with the same fractional bandwidth would have an insertion loss of 6dB. Hence it is not advised that the STW approach be pursued for this integrated optics application given the large bandwidth requirement. This technique may, however, proove useful for some integrated optics applications where bandwidth is of less concern and deeper interaction between the acoustic beam and the optical signal is needed.

The edge-bonded transducer approach is more difficult to fabricate than the STW technique but it provides both low insertion loss at large fractional bandwidth. The edge-bonded transducer technique has been used successfully in applications such as a reflective array compressor (RAC) on ST-Quartz [5]. For this device the reflective array was fabricated on the weakly piezoelectric ST-Quartz substrate to utilize its low temperature coefficient of delay and a thickness-mode $LiNbO_3$ transducer was bonded to the end of the substrate. This makes it possible to build low insertion loss, large bandwidth devices on weakly piezoelectric substrates such as ST-Quartz and GaAs. For the

integrated optics device proposed herein, we can use the non-piezoelectric glass BK-7 and generate the acoustic wave using a thickness mode $LiNbO_3$ transducer.

The edge-bonded transducer configuration used to excite surface waves is shown in Figure 2 where transducer is X-cut $LiNbO_3$. This transducer generates a pure shear wave polarized 41^o from the the Y-axis. For efficient generation of a SAW this shear wave is oriented normal to the substrate surface and the electrode width is on the order of the SAW wavelength. To date there have been no reported attempts to use the edge-bonded transducer technique to generate a STW and as such the effort proposed will be novel in this regard. The proposed design will be to orient the pure shear of the $LiNbO_3$ parallel to the substrate surface rather than normal to it. Whereas the electrode width for efficient SAW generation was an acoustic wavelength, the electrode width for STW generation will be approximately 10 acoustic wavelengths. This is merely an estimate and the optimum design will have to be established experimentally and theoretically during the research effort.

For SAW applications the edge-bonded transducer technique has been used to achieve fractional bandwidths of 91% at 100MHz while obtaining single-transducer conversion losses of 4dB [6]. It is expected that the edge-bonded transducer used to generate STW will be of comparable bandwidth and insertion loss. To make an estimate of the power required for each edge-bonded transducer one can make an analogy to bulk acousto-optic technology.

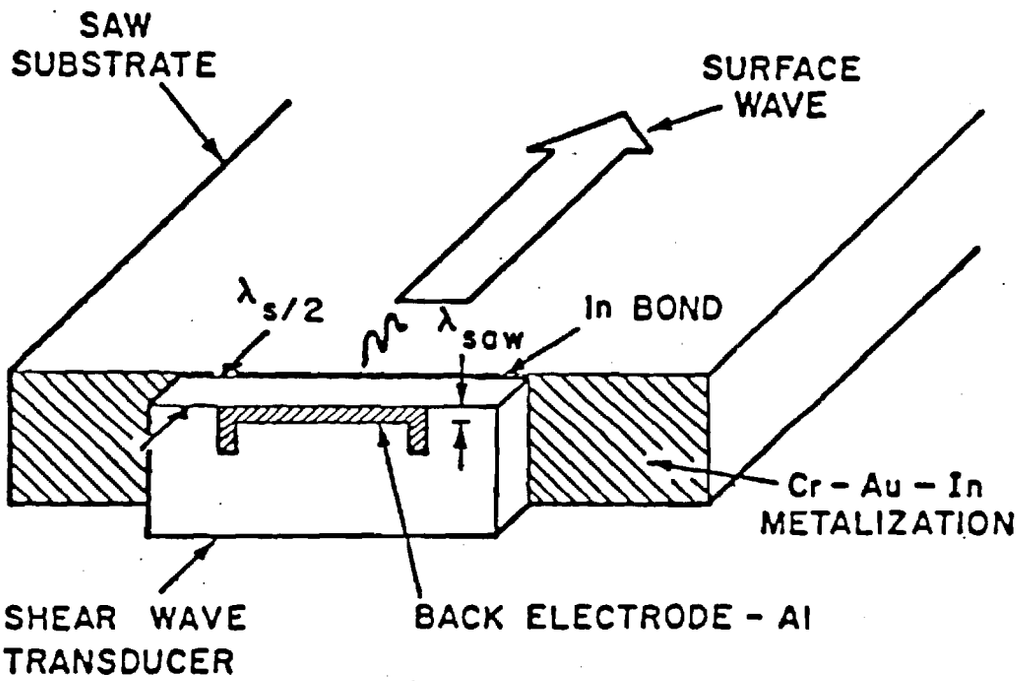

Figure 2: Edge-bonded transducer configuration

Typical conversion loss for a transducer for a bulk acousto-optic device is 3dB and approximately 1 Watt of RF power is required to modulate an optical beam with a cross sectional area of 2 or 3 mm^2. Since the approach described herein is similar to the bulk case we can proceed by considering that for the bulk case a power density of 500mW/mm^2 is required for 100% modulation. The interaction area for the case described herein will be 50um by 1 mm such that instead of 1Watt per transducer, only 25mW per transducer will be required. The total power then required for the 8-transducer switch will be approximately 200mW.

Since these transducers are to be bonded to the BK-7 glass substrate in a slot rather than at the end of the substrate a word should be said about the proposed fabrication technique which is outlined in Figure 3. First the 10-wavelength wide Al electrode will be deposited onto the $LiNbO_3$ and that side of the $LiNbO_3$ piece will be bonded to a glass piece with wax. The $LiNbO_3$ will then be polished to the desired thickness ($\lambda_s/2$). Next, chrome, gold and indium will be evaporated onto both the exposed surface of the $LiNbO_3$ and the slot surface where the transducer is to be bonded. Following this the $LiNbO_3$-glass piece should be pressure bonded to the BK-7 substrate. Finally, the glass backing should be removed by heating the device to a temperature where the wax melts but the chrome-gold-indium bond holds. Next, wire bonds are made to the transducer electrode and the chrome-gold-indium layer and acoustically the device is ready for operation. This is a proposed fabrication procedure and

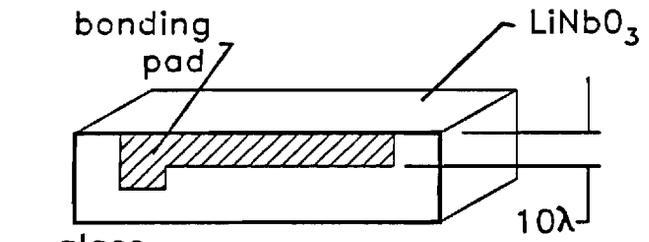

- Evaporate electrode on $LiNbO_3$

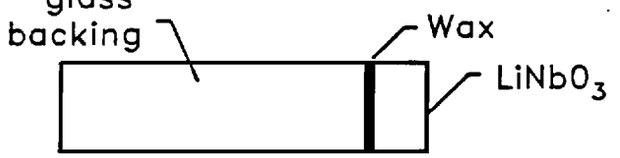

- Affix $LiNbO_3$ piece to glass with wax and polish to desired thickness ($\lambda_s/2$)

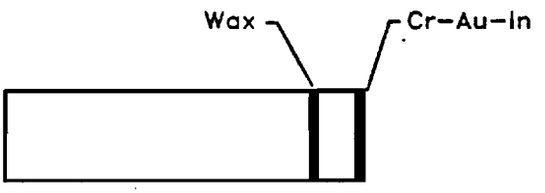

- Evaporate Cr–Au–In in layers on $LiNbO_3$

- Evaporte Cr–Au–In in layers on BK–7 in slot

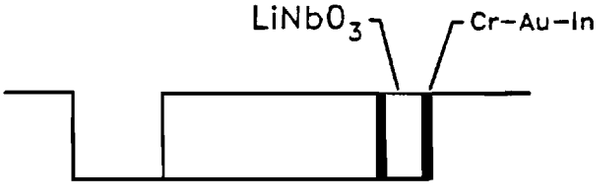

- Pressure bond $LiNbO_3$ to BK–7

- Elevate temperature to melt wax and remove glass backing, remove excess wax with solvent

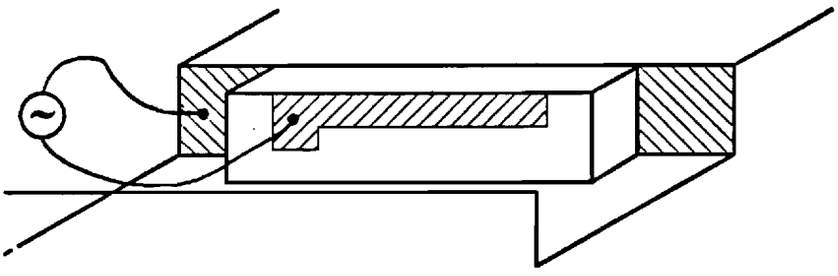

- Wirebond to transducer

Figure 3: Proposed fabrication steps for LiNbO3 edge-bonded transducers on slotted BK-7

represents a best estimate of what will be required. Further research will be needed to work out the fabrication details.

References

[1] B.A. Auld and D.F. Thompson, "Temperlature compensation of surface transverse waves for stable oscillator applications," to be published in the 1987 IEEE Ultrasonics Symposium Proceedings.

[2] D.F. Thompson and B.A. Auld, "Surface transverse wave propagation under metal strip gratings," 1986 IEEE Ultrasonics Symposium Proceedings, pp. 261-266.

[3] A. Ronnelkleiv, "High-Q resonators based on surface transverse waves," 1986 IEEE Ultrasonics Symposium Proceedings, pp 257-260.

[4] C.A. Flory and R.L. Baer, "Surface transverse wave mode analysis and coupling to interdigital transducers," to be published in 1987 IEEE Ultrasonics Symposium Proceedings.

[5] W.D. Hunt, E.H. Young, and M.L. Shah, "The edge-bonded ST-Quartz reflective array FM flilter," presented at the 1978 Ultrasonics Symposium but not published in the proceedings.

[6] D.E. Oates and R.A. Becker, "LiNbO3 surface acoustic wave edge-bonded transducers on ST-Quartz and ,001>-cut GaAs," 1980 IEEE Ultrasonics Symposium Proceedings, pp. 367-370.

[7] C. Lardat and P. Defranould, "Applications of edge-bonded tranducers to SAW components," Proceedings of the IEEE, vol. 64, p. 637, 1976.

[8] K.H. Yen, K.F. Lau, and R.S. Kagiwada, "Energy-trapped shallow bulk acoustic waves," Electronics Letters, vol. 15, p. 206, 1979.